

Hydrothermal Synthesis of ZnO Nanorods in the Diameter Regime of 50 nm

Bin Liu and Hua Chun Zeng*

Department of Chemical and Environmental Engineering, Faculty of Engineering, National University of Singapore, 10 Kent Ridge Crescent, Singapore 119260

Received December 28, 2002; E-mail: chezhc@nus.edu.sg

ZnO is an important electronic and photonic material because of its wide direct band gap of 3.37 eV. In recent years, in particular, ultraviolet lasing from ZnO nanostructures has been demonstrated at room temperature,^{1,2} which triggers a wide range of subsequent research in searching for newer synthetic methods. There have been many existing preparative techniques for this material.^{1–17} Among them, a vapor-phase transport process with the assistance of noble metal catalysts and thermal evaporation are the two major vapor methods to fabricate one-dimensional ZnO nanostructures (nanorods) with controllable diameters.^{1–9} In addition to these techniques, it is well conceived that preparation of ZnO via solution chemical routes provides a promising option for large-scale production of this material. Although they have long been used for ZnO single-crystal growth,^{11,12} wet-chemical approaches still face the problems of polydispersity and difficulties in bringing the rod diameters down to the sub-100 nm regime.^{11–16} Very recently, single-crystalline ZnO nanorods have been prepared with a modified microemulsion method.¹⁶ Although the regularity of the rod-shape has been significantly improved, the achieved rod diameter is still in the range of 150 nm with that wet-chemical method.¹⁶ In this communication, we will report a novel wet-chemical approach for the preparation of monodispersed ZnO nanorods with a significant advance in bringing down the average diameter to the regime of smaller than 50 nm and bringing up the aspect ratio to 30–40.

The alkali solution of zinc was prepared by dissolving 14.87 g of zinc nitrate [$\text{Zn}(\text{NO}_3)_2 \cdot 6\text{H}_2\text{O}$] and 40.00 g of NaOH in deionized water to form a 100.0 mL solution ($[\text{Zn}^{2+}] = 0.50 \text{ M}$, $[\text{OH}^-] = 10.00 \text{ M}$; molar ratio of $\text{Zn}^{2+}:\text{OH}^- = 1:20$). Three milliliters of the above solution was then mixed with 0.0–5.0 mL of deionized water and 25.0–30.0 mL of pure alcohol ($\text{C}_2\text{H}_5\text{OH}$), followed by adding 5.0–6.0 mL of ethylenediamine ($\text{C}_2\text{H}_4(\text{NH}_2)_2$, EDA; molar ratio of $\text{Zn}^{2+}:\text{EDA} = \text{ca. } 1:50$ to $1:60$). Before being transferred to a Teflon-lined autoclave, the solution mixture was pretreated under an ultrasonic water bath for 20–40 min. The hydrothermal syntheses were conducted at 180 °C for 20 h in an electric oven. After the reactions, white crystalline products (ZnO nanorods) were harvested by centrifugation and thorough washings with deionized water. The obtained ZnO nanorods were characterized with scanning electron microscopy, energy-dispersive X-ray spectroscopy (SEM/EDX, JSM-5600LV), transmission electron microscopy, selected area electron diffraction (TEM/SAED, JEM-2010F, and HRTEM, Philips FEI-CM200), and powder X-ray diffraction (XRD, Shimadzu XRD-6000, Cu $\text{K}\alpha$ radiation).¹⁸

As reported in Figure 1, the ZnO nanorods (in 100% morphological yield) were arranged in the form of bushlike assembly with the well-faceted $\langle 0001 \rangle$ ends projecting out. The calculated mean diameter and length of these rods are 45.6 nm (population standard deviation $\sigma = 13.0 \text{ nm}$) and 1.54 μm (population standard deviation $\sigma = 0.16 \mu\text{m}$; based on SEM/TEM images, not shown), respectively. An exceptionally large aspect ratio is thus achieved in the range of 30–40. Furthermore, each nanorod has a uniform diameter

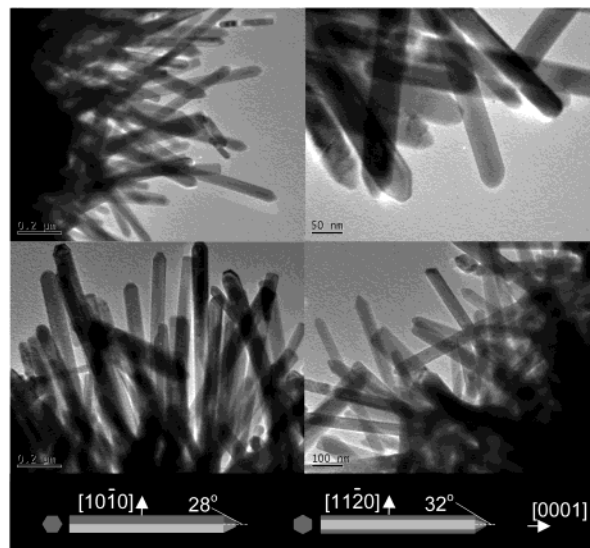


Figure 1. TEM images of ZnO nanorods synthesized in the current work (3.0 mL of alkali Zn^{2+} solution + 5.0 mL of H_2O + 25.0 mL of $\text{C}_2\text{H}_5\text{OH}$ + 5.0 mL of $\text{C}_2\text{H}_4(\text{NH}_2)_2$; 180 °C, 20 h) with different magnifications. Some crystals end with $-c$ termination (the flatten ends), although the majority of the crystals in this figure have $+c$ ends. Inset: schematic illustrations of growing $+c$ ends of ZnO with two common interplanar angles.

along its entire length, indicating the growth anisotropy in the $+c$ -axis is strictly maintained throughout the process. In particular, no branching is observed, which implies that the ZnO nanorods were grown from spontaneous nucleation with high crystal perfection. Indeed, crystal boundaries of the rods are well defined, and the fast growing ends are clearly bounded by seven crystallographic facets, (10-11), (01-11), (-1011), (0-111), (1-101), (-1101), and (0001), on the basis of known interplanar angles (inset, Figure 1).

On the basis of the XRD results (Figure 2a), the crystallographic phase of these ZnO nanorods belongs to the Wurtzite-type (SG: $P6_3mc$), and the measured lattice constants of c_0 and a_0 of this hexagonal phase are 5.21 and 3.25 Å, respectively ($c_0/a_0 = 1.60$). Although the majority of ZnO nanorods were assembled into the bushlike aggregates (Figure 1), individual nanorods can be separated with sonication. All separated ZnO nanorods show two well-faceted crystal ends along the $\pm c$ -axis. Furthermore, ZnO nanorods projecting out with predominant $-c$ termination can also be observed in this type of aggregation (see Supporting Information). Because the $-c$ axis is the slowest growth direction, the above results confirm that the nanorods were not nucleated and grown on the same solid supports in the aggregates.

Instead, they were individually grown from the spontaneous nucleation, which then formed the final assemblies. Figure 2b,c shows a free-standing ZnO nanorod and its related SAED pattern. The diffraction pattern can be indexed as [1-100] zone spots, and excellent single crystallinity is thus elucidated. The chemical

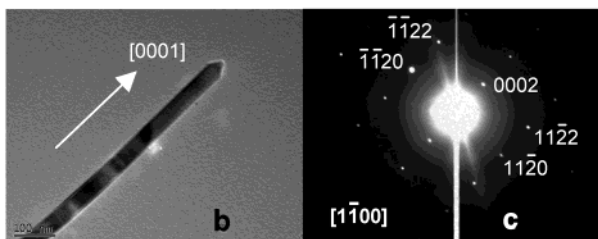
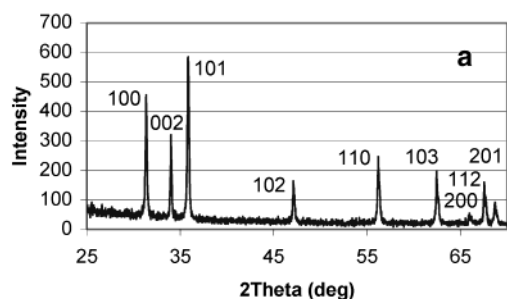


Figure 2. (a) XRD pattern of the as-prepared ZnO nanorods, (b) TEM image of a free-standing ZnO nanorod, and (c) SAED pattern of the nanorod in (b).

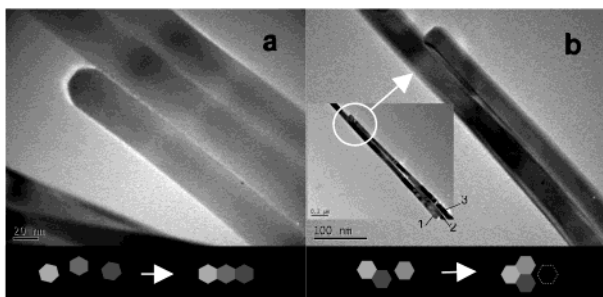


Figure 3. TEM images of (a) three ZnO nanorods attached with their side wall planes, and (b) coupling of two ZnO nanorods via a bending attachment process (the small scale bar in the inset equals 0.2 μm). Insets: schematic illustrations (axial views in the [0001] direction of the rods) of the coplanar attachment in (a), and the “fly over” attachment in (b).

stoichiometry of ZnO nanorods was investigated with EDX, which indeed gave an atomic ratio of Zn:O \approx 1:1.

The excellent crystallinity of the ZnO nanorods is also reflected in the coupling among the as-grown ZnO nanorods. As elucidated in Figure 3, a small number of detached nanorods underwent a multiplying growth via a “cementing mechanism” (a larger crystal was grown from direct combination of small crystals; also called “oriented attachment”)^{17,18} under the same processing conditions of Figure 1 (e.g., 180 °C, 20 h). The observed long-range attachment among the individual crystals reveals that there exist smooth prismatic side planes of the rods: (10-10), (01-10), (-1010), (0-110), (1-100), and (-1100). Under the hydrothermal conditions, the side crystal planes were able to glue together to form a larger crystal. In Figure 3a, three nanorods are arranged in a coplanar manner using their side planes parallel to the incident electron beam, while in Figure 3b a third ZnO nanorod (circled top portion) is attached to the first one from the upper right-hand-side, although there is a second rod in between. This indicates that the long ZnO nanorods are flexible enough to turn around for this type of crystal coupling.

The lattice continuity among attached crystals has been confirmed by SAED/HRTEM results (see Supporting Information).

Regarding the growth process, it is believed that the ultrasonic pretreatment of the solution mixture is an important step prior to the hydrothermal reactions at 180 °C, which may generate a suitable amount of ZnO cluster nuclei for the subsequent hydrothermal growth. Without this pretreatment, the observed uniform nanorod morphology simply cannot be attained. For example, much larger and shorter ZnO rods and particles had been generated from the untreated precursor solution (with the same composition as that of Figure 1) after only 2 h reactions at 180 °C (see Supporting Information). Furthermore, the usages of a high basic condition and an alcoholic environment are the two crucial keys in ensuring the formation of ZnO_2^{2-} and a controlled release of this species from the alcohol–water mixture phase to the growing ZnO nanostructures. On the other hand, the EDA present may serve as adsorbing (chelating) ligands to the Zn^{2+} cations (primarily on the six prismatic side planes), inhibiting the radial enlargement of the rods. A more detailed investigation on the precursor solution and solution–solid chemistries is currently in progress.

In summary, we have developed a novel wet-chemical method to prepare monodispersed ZnO nanorods with high crystallinity in the diameter regime of 50 nm with exceptionally large aspect ratios. This simple approach should promise us a future large-scale synthesis of this nanostructured material for many important applications in nanotechnology in a controlled manner.

Acknowledgment. The authors gratefully acknowledge the financial support of the Ministry of Education and the National Science and Technology Board, Singapore.

Supporting Information Available: TEM images (PDF). This material is available free of charge via the Internet at <http://pubs.acs.org>.

References

- (1) Tang, Z. K.; Wong, G. K. L.; Yu, P.; Kawasaki, M.; Ohtomo, A.; Koinuma, H.; Segawa, Y. *Appl. Phys. Lett.* **1998**, *72*, 3270.
- (2) Huang, M. H.; Mao, S.; Feick, H.; Yan, H.; Wu, Y.; Kind, H.; Webber, E.; Russo, R.; Yang, P. *Science* **2001**, *292*, 1897.
- (3) Huang, M. H.; Wu, Y.; Feick, H.; Tran, N.; Weber, E.; Yang, P. *Adv. Mater.* **2001**, *13*, 113.
- (4) Johnson, J. C.; Yan, H.; Schaller, R. D.; Haber, L. H.; Saykally, R. J.; Yang, P. *J. Phys. Chem. B* **2001**, *105*, 11387.
- (5) Pan, Z. W.; Dai, Z. R.; Wang, Z. L. *Science* **2001**, *291*, 1947.
- (6) Gao, P.; Wang, Z. L. *J. Phys. Chem. B* **2002**, *106*, 12653.
- (7) Yao, B. D.; Chan, Y. F.; Wang, N. *Appl. Phys. Lett.* **2002**, *81*, 757.
- (8) Hu, J. Q.; Li, Q.; Wong, N. B.; Lee, C. S.; Lee, S. T. *Chem. Mater.* **2002**, *14*, 1216.
- (9) Lao, J. Y.; Wen, J. G.; Ren, Z. F. *Nano Lett.* **2002**, *2*, 1287.
- (10) Liu, R.; Vertegel, A. A.; Bohannon, E. W.; Sorenson, T. A.; Switzer, J. A. *Chem. Mater.* **2001**, *13*, 508.
- (11) Li, W.-J.; Shi, E.-W.; Zhong, W.-Z.; Yin, Z.-W. *J. Cryst. Growth* **1999**, *203*, 186.
- (12) Wenisch, H.; Kirchner, V.; Hong, S. K.; Chen, Y. F.; Ko, H. J.; Yao, T. *J. Cryst. Growth* **2001**, *227–228*, 944.
- (13) Zhang, J.; Sun, L.; Yin, J.; Su, H.; Liao, C.; Yan, C. *Chem. Mater.* **2002**, *14*, 4172.
- (14) Choi, K.-S.; Lichtenegger, H. C.; Stucky, G. D.; McFarland, E. W. *J. Am. Chem. Soc.* **2002**, *124*, 12402.
- (15) Tian, Z. R.; Voigt, J. A.; Liu, J.; Mckenzie, B.; Mcdermott, M. J. *J. Am. Chem. Soc.* **2002**, *124*, 12954.
- (16) Guo, L.; Ji, Y. L.; Xu, H.; Simon, P.; Wu, Z. *J. Am. Chem. Soc.* **2002**, *124*, 14864.
- (17) Pacholski, C.; Kornowski, A.; Weller, H. *Angew. Chem., Int. Ed.* **2002**, *41*, 1188.
- (18) Sampanthar, J. T.; Zeng, H. C. *J. Am. Chem. Soc.* **2002**, *124*, 6668.

JA0299452